J. Phys. B: At. Mol. Opt. Phys. **44** (2011) 225503 (6pp) doi:10.1088/0953-4075/44/22/225503

Angular momentum and two-photon detuning dependence of reflection spectrum on degenerate two-level systems in Cs vapour

Haitao Zhou, Miaojun Guo, Dan Wang, Jiangrui Gao and Junxiang Zhang

The State Key Laboratory of Quantum Optics and Quantum Optics Devices, Institute of Opto-Electronics, Shanxi University, Taiyuan 030006, People's Republic of China

E-mail: junxiang@sxu.edu.cn

Received 2 September 2011, in final form 4 October 2011
Published 1 November 2011
Online at stacks.iop.org/JPhysB/44/225503

Abstract

The absorption and reflection spectrum of probe light, interacting with a degenerate two-level system of any transition in the Cs D1 line driven by standing-wave, is experimentally studied. The effect that absorption changes from a transparency dip to an absorption peak when the travelling coupling field is replaced by the standing-wave field can only occur in the hyperfine transition $F_g \leftrightarrow F_e \leqslant F_g$ (F_g and F_e are the total angular momentum of the ground and the excited levels respectively), and in this case, a reflection of probe can be generated. It is also examined that the absorption coefficient and reflection efficiency in the transition of $F_g > F_e$ are much higher than that in $F_g = F_e$. For the transition of $F_g < F_e$, where coherent population trapping cannot be established, the absorption does not change the sign, and there is no reflection to be observed when the coupling is switched from a travelling to a standing-wave field. As a consequence, only the degenerate two-level systems, where the population is trapped in the ground states, can exhibit steep absorption and reflection of the probe light with a standing-wave coupling. Furthermore, the reflection spectra with an asymmetric profile as the function of one- and two-photon detunings are obtained, which is theoretically explained by the phase mismatch compensation during the process of four-wave mixing in an atomic system. This shows that under the condition of coherent population trapping the nonlinear reflection can be improved with one- and two-photon detunings in a degenerate two-level system.

(Some figures in this article are in colour only in the electronic version)

1. Introduction

Atomic coherence is an important physical process in quantum optics; it can produce interesting phenomena. For instance, in a Λ-type three-level system, the coherence between the two ground states induced by a two-photon process leads to a coherent population trapping (CPT) [1] and electromagnetically induced transparency (EIT) [2]. In a Doppler-broadened Λ-type three-level EIT system, if the travelling-wave (TW) coupling field is replaced by a standing wave (SW), the absorption of probe light changes from transparency to steep absorption [3]; meanwhile the probe light is reflected or diffracted by the atomic medium [4–6]. This effect, also called electromagnetically induced grating (EIG), has wide applications in all optical switching [4], creation of a stationary light pulse (SLP) [7, 8], manipulation of light propagation to create a tunable photonic bandgap [9, 10] and four-wave mixing (FWM) [8, 11].

The FWM in degenerate two-level systems interacting with TW fields has been widely investigated both

experimentally and theoretically [12–15]. It has been shown that CPT and EIT played an important role in the process of atomic-vapour FWM. And for the degenerate two-level system driven by the SW, the EIT-based FWM can also be viewed as a nonlinear grating formed by the spatially modulating strong SW coupling beam [5–9]. Consequently, the Bragg diffraction of a probe light in the degenerate two-level system has been theoretically discussed [16], and experimentally demonstrated in an atomic beam [17] and cold atoms [18, 19]; the diffraction efficiency below 1% is relatively lower than the obtained reflection efficiency of 10% in cold four-level atoms [11], 7% in three-level hot vapour [4] and 80% in a three-level atomic cell with buffer gas [7].

In this paper, we experimentally investigate the reflection of probe light in a degenerate two-level system of all four transitions in the Cs D1 line of a vapour cell driven by the SW field, and demonstrate that the reflection of EIG can be observed only for the transition of $F_g \geqslant F_e$, in which the ground state population trapping can be established when it is coupled with TW fields [20]. And for the transition of $F_g < F_e$, in which the electromagnetically induced absorption (EIA, the opposite effect of EIT) can be established when it is coupled with TW fields [21], the similar effect of reflection cannot be found. We compare the efficiency of reflection for all the transitions and find that the reflection in $F_g > F_e$ is more efficient than that in other transitions. Further experiments on the absorption of the probe light show that the reflection of the probe light is accompanied by a transformation from EIT with a TW to high absorption with a SW in the two-level system of $F_g \geqslant F_e$. In theory, we give the qualitative explanation of the generated signal of reflection from the FWM process, and find an off one- or two-photon resonance enhancement of reflection. Therefore, up to 80% efficiency can be obtained at a temperature vapour of 60 °C.

2. Experimental setup

Figure 1 shows the relevant energy levels of D1 line of the ^{133}Cs atom; the ground state ($6^2S_{1/2}$) and the excited state ($6^2P_{1/2}$) include two hyperfine structures, whose frequency intervals are 9.192 and 1.168 GHz, respectively. Note that the excited state hyperfine splitting is larger than the Doppler linewidth at room temperature: $\Delta\nu_D \approx 370$ MHz. So that the influence of an additional excited level on the reflection coefficient is neglected [22]. The three types of degenerate structures are: (1) $F_g > F_e$, (2) $F_g = F_e$ and (3) $F_g < F_e$; the total angular momentums are seen in figure 1. The solid lines show the standing-wave coupling fields which are locked near the relevant transitions in the experiment, and the dashed lines denote the probe lights, which are scanned hundreds of million hertzs at the centre of the transitions.

Figure 2 shows the schematic diagram of the experimental arrangement. A grating-feedback external-cavity diode laser (Toptica DL100) with the linewidth of ∼1 MHz is used as the probe field. The Ti: sapphire laser (Coherent MBR110) with the linewidth of 75 kHz is used as the coupling field. The experiment is performed in a Cs cell with anti-reflection-coated end windows (length of 7.5 cm, diameter of 2.5 cm), which

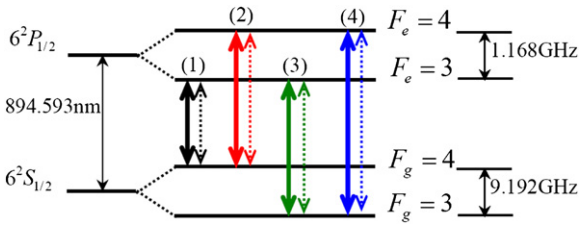

Figure 1. Relevant degenerate two-level system of Cesium D1 line. (1) $F_g = 4 \leftrightarrow F_e = 3$ (black lines), (2) $F_g = 4 \leftrightarrow F_e = 4$ (red lines), (3) $F_g = 3 \leftrightarrow F_e = 3$ (green lines) and (4) $F_g = 3 \leftrightarrow F_e = 4$ (blue lines). The solid lines and the dotted lines represent SW coupling and probe fields, respectively.

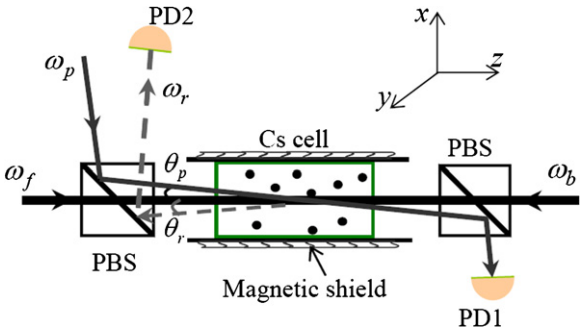

Figure 2. Schematic diagram of experimental arrangement. PBS cube; PD1 and 2, photon detectors. ω_p, ω_f, ω_b and ω_r represent probe, forward coupling, backward coupling and reflected signals, respectively.

is shielded against external magnetic fields by three layers of μ-metal. The e^{-2} full width of probe and coupling beams are 0.5 and 0.67 mm, respectively. The probe is polarized perpendicular to the coupling fields in the cell. In order to avoid the influence of coupling fields on the detection, the probe and forward coupling beam (along the z-direction shown in figure 2) are incident to the cell centre with an angle of $\theta = 0.14°$ ($\theta_p = \theta_r = \theta$). A backward coupling field propagates along the inverse z-axis and is collinear with the forward coupling field so as to form the SW.

The atomic transition frequency is defined as $\omega_{ge}(g, e = 3, 4)$; the frequencies of forward and backward coupling fields are ω_f and ω_b, respectively. As the forward and backward coupling fields come from one laser, we have $\omega_f = \omega_b = \omega_c$. The frequency of probe is ω_p, and the frequency of reflection signal is ω_r. Correspondingly, $\Delta_c = \omega_c - \omega_{ge}$ is defined as the coupling frequency detuning, and $\Delta_p = \omega_p - \omega_{ge}$ is the probe frequency detuning. As ω_r is equal to ω_p due to the condition of energy conservation and phase matching, so the reflected signal-frequency detuning Δ_r is equal to Δ_p. The powers of forward, backward coupling fields, probe and reflection are represented by P_f, P_b, P_p and P_r, respectively. We define the reflection efficiency as $\eta = (P_r/P_p) \times 100\%$.

3. Experimental results

The detection of the probe absorption coefficient α as a function of probe detuning is firstly made by scanning the probe frequency, meanwhile keeping the coupling SW light at resonant $\Delta_c = 0$, see figure 3. The gray lines in

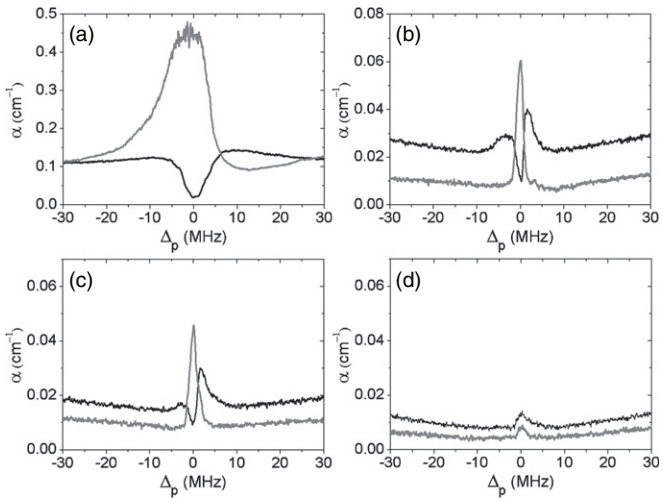

Figure 3. The absorption spectrum of the probe light versus probe frequency detuning for different transitions: (a) $F_g = 4 \leftrightarrow F_e = 3$, (b) $F_g = 4 \leftrightarrow F_e = 4$, (c) $F_g = 3 \leftrightarrow F_e = 3$ and (d) $F_g = 3 \leftrightarrow F_e = 4$. The experimental parameters are: $P_p = 90\ \mu$W, $P_f = 20$ mW, $P_b = 20$ mW (gray lines) and $P_b = 0$ (black lines), $\Delta_c = 0$, $\theta = 0.14°$, $T = 43\ °$C.

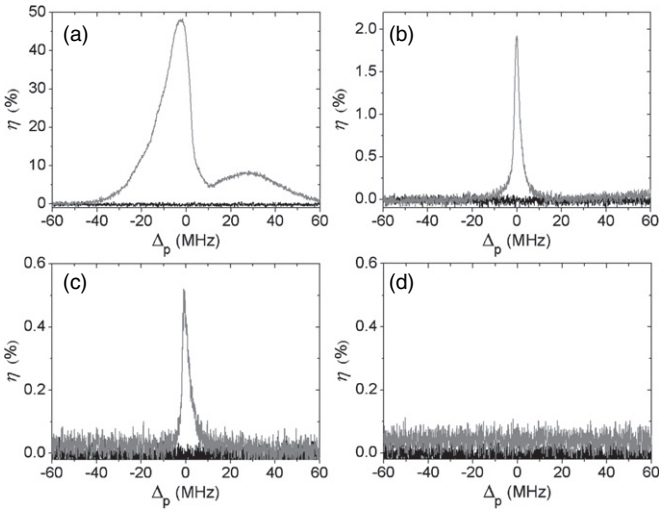

Figure 4. The spectrum of the reflection signal versus the probe frequency detuning for different transitions: (a) $F_g = 4 \leftrightarrow F_e = 3$, (b) $F_g = 4 \leftrightarrow F_e = 4$, (c) $F_g = 3 \leftrightarrow F_e = 3$ and (d) $F_g = 3 \leftrightarrow F_e = 4$. The experimental parameters are the same as that in figure 3.

figure 3 represent the absorption of probe with the SW, and the black lines are the absorption of probe with the TW when the backward coupling beam is blocked.

For the transition $F_g = 4 \leftrightarrow F_e = 3$, see figure 3(a), a high absorption peak (gray line in figure 3(a)) is obtained at the detector of PD1 when both the forward and backward coupling fields are applied to form a SW, and meanwhile, a signal is generated in the direction of reflection, detected by PD2; see the gray line in figure 4(a). However, when only a travelling forward coupling field is applied by blocking the backward coupling, the absorption peak is transformed into a transparency dip (black line in figure 3(a)) at PD1; it causes the reflection signal to disappear completely; see black line in figure 4(a). Similarly, for the transitions $F_g = 4 \leftrightarrow F_e = 4$ and $F_g = 3 \leftrightarrow F_e = 3$, the transformation from EIT to narrow absorption can also be observed when a TW coupling is replaced by a SW coupling (see figures 3(b), (c)), and in this case, a reflection signal is also generated (see figures 4(b), (c)).

Different from the transition of $F_g \geqslant F_e$, as for the transition $F_g = 3 \leftrightarrow F_e = 4$, a small absorption peak for the probe light can be found with the TW coupling [21] or SW coupling. The absorption does not change its sign when a TW is replaced by a SW; see figure 3(d). Furthermore, in figure 4(d), there is no reflection observed by PD2.

A comparison of the relative peak intensities of absorption and reflection spectra among three different transitions of $F_g \geqslant F_e$, including $F_g = 4 \leftrightarrow F_e = 3$, $F_g = 4 \leftrightarrow F_e = 4$ and $F_g = 3 \leftrightarrow F_e = 3$, reveals that higher reflection efficiency is accompanied with the higher absorption, and the reflection is much efficient for the case of $F_g = 4 \leftrightarrow F_e = 3$, in which the reflection efficiency reaches 48% of the total input probe power; the maximum efficiency is about 1.8% for the transition $F_g = 4 \leftrightarrow F_e = 4$ and it is about 0.5% for $F_g = 3 \leftrightarrow F_e = 3$. And on the other hand, the comparison of these effects between $F_g \geqslant F_e$ and $F_g < F_e$ also shows obviously that the reflection of EIG or FWM can only occur for this case of $F_g \geqslant F_e$, in which coherent dark states of the ground sublevels, i.e. CPT can be realized [20, 23]; for example, for the transition $F_g = 4 \leftrightarrow F_e = 3$, two systems of CPT schemes with Λ-links are formed, one denoted with solid black lines for the coherent dark state $\phi_1 = \sqrt{1/128}\{|-4\rangle - \sqrt{28}|-2\rangle + \sqrt{70}|0\rangle - \sqrt{28}|2\rangle + |4\rangle\}$ and the other with dashed gray lines for $\phi_2 = \sqrt{1/16}\{|-3\rangle - \sqrt{7}|-1\rangle + \sqrt{7}|1\rangle - |3\rangle\}$, see figure 5(a). Therefore, the transmission of probe is transparent under the two-photon resonant condition with the TW coupling (black line in figure 3(a)), and it is the superposition of two Λ-type sublevel's action. For the transition $F_g = 4 \leftrightarrow F_e = 4$,a Λ-link of CPT is formed with $\phi_3 = \frac{1}{16}\{\sqrt{70}|-4\rangle - 2\sqrt{10}|-2\rangle + 2\sqrt{9}|0\rangle - 2\sqrt{10}|2\rangle + \sqrt{70}|4\rangle\}$ (see solid black lines in figure 5(b)) and the other V-link of CPT is formed in excited states, but it has strong relaxation losses because of high relaxation of excited states (see the dashed gray lines in figure 5(b)). For the transition $F_g = 3 \leftrightarrow F_e = 3$, it contains a Λ-link CPT $\phi_4 = \frac{1}{4}\{\sqrt{5}|-3\rangle - \sqrt{3}|-1\rangle + \sqrt{3}|1\rangle - \sqrt{5}|3\rangle\}$ and V-link of coherent dark states; the effect is similar to that of the transition $F_g = 4 \leftrightarrow F_e = 4$. However, for the transition $F_g = 3 \leftrightarrow F_e = 4$, only V-links of CPT can be formed (see the dashed black and dashed gray lines in figure 5(d)), which cannot lead to a steady CPT resonance because of the high relaxation losses of excited states. Instead, a termed EIA effect can be observed because of the spontaneous transformation of the light-induced coherence [21]. So we could deduce qualitatively that the effect of CPT, as well as the transformation (from EIT to narrow absorption), plays a key role for the generation of reflection of EIG.

The efficiency can be enhanced further with the increase of atom numbers via increasing the temperature of the vapour

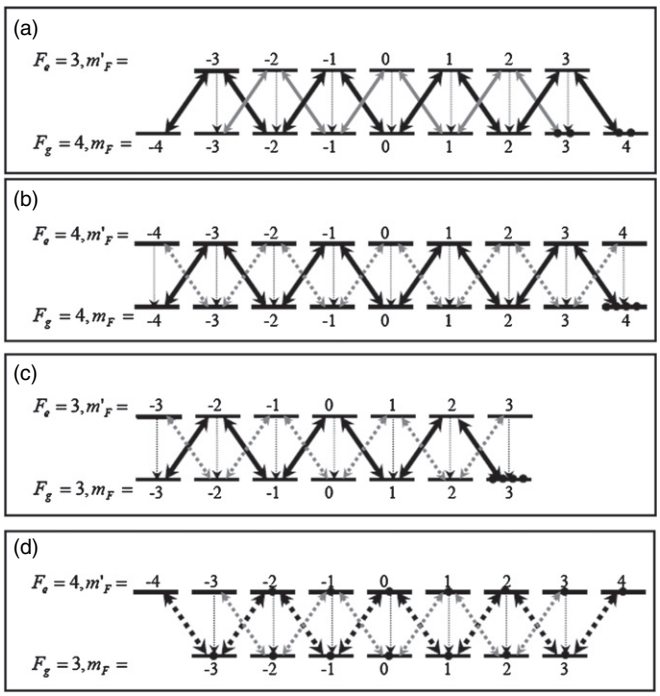

Figure 5. Zeeman sublevels for different degenerate transitions: (a) $F_g = 4 \leftrightarrow F_e = 3$, (b) $F_g = 4 \leftrightarrow F_e = 4$, (c) $F_g = 3 \leftrightarrow F_e = 3$ and (d) $F_g = 3 \leftrightarrow F_e = 4$.

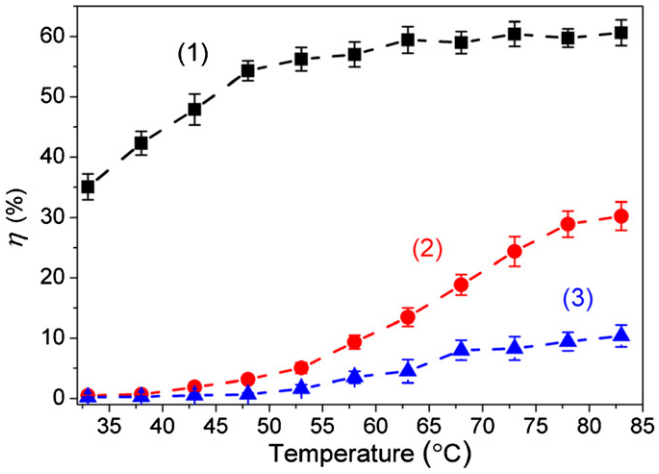

Figure 6. The reflection efficiency versus the temperature of Cs cell at $\Delta_c = 0$ for different transitions: (1) $F_g = 4 \leftrightarrow F_e = 3$ (black square), (2) $F_g = 4 \leftrightarrow F_e = 4$ (red circle) and (3) $F_g = 3 \leftrightarrow F_e = 3$ (blue triangle). The other experimental parameters are the same as that in figure 3.

cell. Figure 6 shows the dependence of the reflection efficiency on the temperature of the vapour cell. For the case of $F_g = 4 \leftrightarrow F_e = 3$, it is obviously seen that the reflection efficiency increases from 30% to 60% when the temperature increases from 30 to 80 °C, and it gets saturated at $T = 63$ °C. For the case of $F_g = 4 \leftrightarrow F_e = 4$ and $F_g = 3 \leftrightarrow F_e = 3$, the maximum efficiency is 30% and 10%, respectively.

Moreover, it is also found that the maximum efficiency is obtained at off-resonant one-photon detuning $\Delta_p < 0$; as can be seen in figure 4(a), the reflection spectrum exhibits a

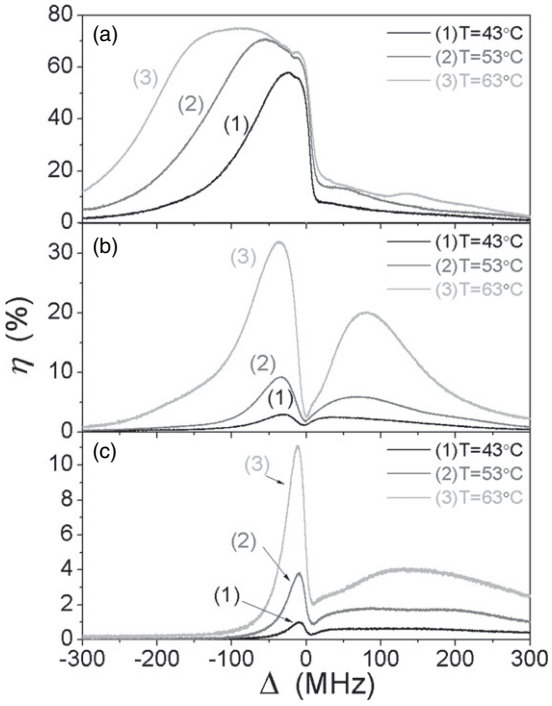

Figure 7. The reflection efficiency versus the two-photon detuning Δ ($\Delta_p = \Delta_c = \Delta$) for different transitions: (a) $F_g = 4 \leftrightarrow F_e = 3$, (b) $F_g = 4 \leftrightarrow F_e = 4$ and (c) $F_g = 3 \leftrightarrow F_e = 3$.

asymmetric profile, which is related to the effect of dispersion compensation of phase mismatching [24] or the refractive index-dependent Bragg condition [10]; the detailed discussion will be shown in the following part. More importantly, the reflection efficiency can be enhanced with two-photon detuning. Figure 7 shows the dependence of efficiency on the two-photon detuning when scanning both the frequencies of probe and coupling fields at the same time. An asymmetric profile is obviously seen, and the efficiency can be improved to be 75% when the temperature increases to $T = 63$ °C at the two-photon detuning $\Delta \sim 100$ MHz. We give the explanation of this effect as follows.

4. The theoretical model

We present in this section a simple theoretical model to mainly discuss the asymmetric spectra of reflection and their enhancement. With respect to the condition of experiment, the model is simplified for both the atomic system and laser fields. It is well known that the population trapping occurs in a degenerate two-level system of $F_g \geqslant F_e$ with a circularly polarized or p-polarized pump laser [25]. As we have described above, in our experiment, when the coupling fields with linear polarization along the x-axis are interacting with the atoms, then they can be seen as p-polarized if we define a quantization axis in the x-direction. Due to the pumping effect by strong p-polarized fields, the atom is trapped in $F_g = 4$, $m_F = \pm 4$ for the two-level of $F_g = 4 \leftrightarrow F_e = 3$, or it is trapped in $F_g = 4$, $m_F = 0$ or $F_g = 4$, $m_F = 0$ for $F_g = 4 \leftrightarrow F_e = 4$ or $F_g = 3 \leftrightarrow F_e = 3$. The probe light whose polarization is perpendicular to the

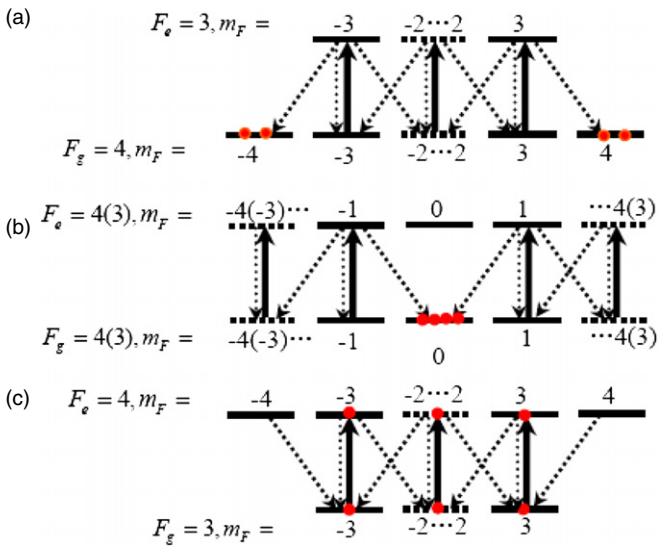

Figure 8. Population trapping in the degenerate system two-level (a) $F_g = 4 \leftrightarrow F_e = 3$ and (b) $F_g = 4 \leftrightarrow F_e = 4$ ($F_g = 3 \leftrightarrow F_e = 3$) transitions driven by p-polarized coupling fields; ground- and excited-state pump-induced populations for the transition of (c) $F_g = 3 \leftrightarrow F_e = 4$ with p-polarized coupling fields. The solid arrows indicate the coupling fields and the dashed arrows indicate spontaneous emission.

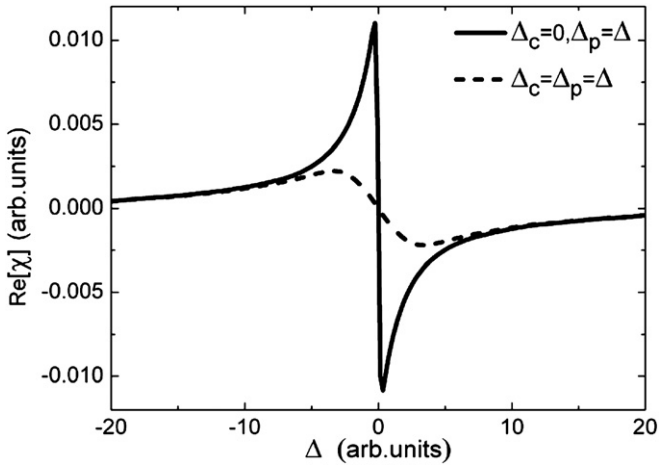

Figure 9. The dispersion of probe as the function of single-photon detuning (solid line) and two-photon detuning (dashed line).

coupling fields can be seen as s_+- and s_--polarized fields. Based on this consideration, the degenerate two-level system $F_g \geqslant F_e$ can be simplified as a pair of three-level systems; see figures 8(a), (b). Thus, the same equations in [24] are used for the theoretical discussion.

Because of the narrow absorption of the probe light in SW coupling, the anomalous dispersion for the probe is thus accompanied; see the solid line in figure 9. The refractive indexes $n_r = n_p = 1 + (1/2)\mathrm{Re}[\chi]$ for both the probe and reflection fields deviate from unit at off-resonant; the value of the wave vector mismatch in the z-direction Δk_z will be

$$\Delta k_z = 2(n_p \omega_p \cos\theta - \omega_c)/c = [2(\omega_p \cos\theta - \omega_c) + \mathrm{Re}[\chi]\omega_p \cos\theta]/c. \quad (1)$$

Note that the first term on the right-hand side of equation (1) is $2(\omega_p \cos\theta - \omega_c)/c < 0$ for the experimental angle $\theta = 0.14°$. However, the second term can cause ΔK_z close to 0 (i.e. compensate the phase mismatching) when $\mathrm{Re}[\chi] > 0$, and on the other hand, $\mathrm{Re}[\chi] < 0$, may further increase the phase mismatching, leading to the efficiency being smaller than that at $\mathrm{Re}[\chi] > 0$; finally it leads to the asymmetric spectrum of reflection in figure 4(a). And the dispersion $\mathrm{Re}[\chi]$ is also plotted in figure 9 (dashed line) as the function of the two-photon detuning. For the two-photon detuning $\Delta < 0$, we still have $\mathrm{Re}[\chi] > 0$, which gives the compensation at $\Delta < 0$, so that an enhancement of reflection is obtained at $\Delta < 0$; see figure 7. Note that the dip in the spectrum of reflection at resonance is partly due to the high absorption of the signal generated by the atoms, which exhibits narrow absorption with the SW in figure 3(a). For the transition of $F_g < F_e$, see figure 8(c), as the atoms cannot be populated completely and steadily with the ground states, no reflection signal is generated for the atom even when coupled by the SW.

It is also seen that the $\mathrm{Re}[\chi]$ for the one-photon detuning is narrower than that for the two-photon detuning, so that compensation occurs in a large range of the two-photon detuning, which in figure 7 gives rise to a wider reflection spectrum than that in figure 4.

5. Conclusions

In summary, we have experimentally investigated the absorption and reflection spectra of the probe field in the degenerate two-level system coupled by strong SW light. We find that only for the transition $F_g \leftrightarrow F_e \leqslant F_g$, the transformation from EIT to EIA and the reflection signal can be observed. We propose the enhancement of reflection efficiency at an off one- or two-photon resonance. In theory, based on the simplified model, the enhancement of reflection was explained as the dispersion compensation of phase mismatching. Owing to the properties, for instance, high reflection efficiency, wide range of detuning of the coupling field without the influence of the original field, the discussion would have many potential applications in quantum optics and quantum information, such as the multi-channel information processing, tuneable optical switching.

Acknowledgments

We gratefully acknowledge Dawei Wang and Shiyao Zhu for discussion and making helpful and important comments. This work is supported in part by the NSFC (nos 10974126, 60821004), National Basic Research Program of China (no 2010CB923102).

References

[1] Arimondo E and Orriols G 1976 *Nuovo Cimento Lett.* **17** 333
[2] Boller K-J, Imamoglu A and Harris S E 1991 *Phys. Rev. Lett.* **66** 2593
[3] Affolderbach C, Knappe S and Wynands R 2002 *Phys. Rev.* A **65** 043810
[4] Brown A W and Xiao M 2005 *Opt. Lett.* **30** 699

[5] Cardoso G C, de Carvalho V R, Vianna S S and Tabosa J W R 1999 *Phys. Rev.* A **59** 1408
[6] Mitsunaga M and Imoto N 1999 *Phys. Rev.* A **59** 4773
[7] Bajcsy M, Zibrov A S and Lukin M D 2003 *Nature* **426** 638
[8] Lin Y, Liao W, Peters T, Chou H, Wang J, Cho H, Kuan P and Yu Ite A 2009 *Phys. Rev. Lett.* **102** 213601
[9] Artoni M and La Rocca G C 2006 *Phys. Rev. Lett.* **96** 073905
[10] Schilke A, Zimmermann C, Courteille P W and Guerin W 2011 *Phys. Rev. Lett.* **106** 223903
[11] Kang H, Hernandez G and Zhu Y F 2004 *Phys. Rev.* A **70** 061804
[12] Villain P, Öhberg P, Santos L, Sanpera A and Lewenstein M 2001 *Phys. Rev.* A **64** 023606
[13] Wang S, Ducreay D G, Pina R, Yan M and Zhu Y 2000 *Phys. Rev.* A **61** 033805
[14] Boyer V, McCormick C F, Arimondo E and Lett P D 2007 *Phys. Rev. Lett.* **99** 143601
[15] Du S, Wen J, Rubin M H and Yin G Y 2007 *Phys. Rev. Lett.* **98** 053601
[16] Pawelec E, Gawlik W, Samson B and Musioł K 1996 *Phys. Rev.* A **54** 913
[17] Do B, Cha J, Elliott D S and Smith S J 1998 *Phys. Rev.* A **58** 3089
[18] Cardoso G C and Tabosa J W R 2002 *Phys. Rev.* A **65** 033803
[19] Gattobigio G L, Michaud F, Javaloyes J, Tabosa J W R and Kaiser R 2006 *Phys. Rev.* A **74** 043407
[20] Smirnov V S, Tumaikin A M and Yudin V I 1989 *Zh. Eksp. Teor. Fiz.* **96** 1613–28
Smirnov V S, Tumaikin A M and Yudin V I 1989 *Sov. Phys.—JETP* **69** 913–21 (Engl. Transl.)
[21] Lezama A, Barreiro S and Akulshin A M 1999 *Phys. Rev.* A **59** 4732
[22] Mishina O S, Scherman M, Lombardi P, Ortalo J, Felinto D, Sheremet A S, Bramati A, Kupriyanov D V, Laurat J and Giacobino E 2011 *Phys. Rev.* A **83** 053809
[23] Milner V, Chernobrod B M and Prior Y 1996 *Europhys. Lett.* **34** 557
[24] Zhang J X, Zhou H T, Wang D W and Zhu S Y 2011 *Phys. Rev.* A **83** 053841
[25] Goren C, Wilson-Gordon A D, Rosenbluh M and Friedmann H 2003 *Phys. Rev.* A **67** 033807